n-Type Charge Transport in Heavily *p*-Doped Polymers

Zhiming Liang,^a Hyun Ho Choi,^{b,} Xuyi Luo,^c Uma Shantini Ramasamy,^{a,e} Tuo Liu,^a J. Andrew Hitron,^f Alex M. Boehm,^a Ashkan Abtahi,^{a,d} Jacob L. Hempel,^g Douglas R. Strachan,^g Jianguo Mei,^c Chad Risko,^{a,e} Vitaly Podzorov,^b and Kenneth R. Graham*^a

Author affiliations

*Corresponding author

^aDepartment of Chemistry, University of Kentucky, Lexington, USA

E-mail: Kenneth.Graham@uky.edu

^b Department of Physics and Astronomy, Rutgers University, Piscataway, New Jersey 08854, USA.

^cDepartment of Chemistry, Purdue University, West Lafayette, USA

^dDepartment of Physics, University of Kentucky, Lexington, USA

eCenter for Applied Energy Research, University of Kentucky, Lexington, USA

^fMH Catalyst, LLC, Lexington, USA

gDepartment of Physics & Astronomy, University of Kentucky, Lexington, USA

Abstract:

It is commonly assumed that charge conduction in doped π -conjugated polymers is dominated by one type of charge carrier, either holes or electrons, as determined by the dopant. However, measurements of Seebeck coefficients and electrical conductivity have led to the suggestion that both carrier types may contribute significantly to charge-carrier transport in these materials. For the first time, we directly show that both positive and negative charge carriers contribute to charge-carrier transport in conjugated polymers that are heavily p-doped with strong electron acceptors. This conclusion is reached through Seebeck coefficient and Hall effect measurements. Specifically, the Seebeck coefficient in several heavily p-doped polymers changes its sign from positive to

⁶ Current address: School of Materials Science and Engineering & Engineering Research Institute, Gyeongsang National University, Jinju 52828, Korea.

negative as the concentration of strongly electronegative FeCl₃ dopant increases, while Hall effect measurements for the same highly *p*-doped polymers reveal that band-like electrons are the dominant charge carriers. Ultraviolet and inverse photoelectron spectroscopy measurements, supported by density functional theory calculations, show that doping with electron acceptors modifies the electronic structure of the polymers, leading to the densities of unoccupied and occupied states converging at high doping concentrations. This convergence of the density of states explains the presence of electrons and holes moving in the unoccupied or occupied manifolds of electronic states, respectively, as observed in this work. We show that the generation of both mobile electrons and holes can provide a route to achieving high-performing *n*-type organic thermoelectrics through heavy *p*-type doping.

Introduction

Charge-carrier transport in π -conjugated polymers (CPs) has been a subject of intense interest since the discovery of electrically conductive polymers half a century ago, ¹⁻⁴ with the reported transport mechanisms ranging across metallic, ^{2, 3, 5-8} semimetallic, ⁹ and hopping-type regimes. ^{3, 10-13} Here, metallic and semi-metallic regimes suggest a band-like transport mechanism with the Fermi energy (E_F) lying within one band of electronic states for a metal, or at the intersection of two bands of electronic states for a semi-metal. ⁹ Charge carriers in amorphous, paracrystalline, and most semi-crystalline polymers tend to be kinetically limited by a hopping-type transport. By contrast, in a few highly crystalline polymers band-like transport can occur either through a metallic or semi-metallic density of states (DOS) distribution. ^{8, 9} Furthermore,

in highly doped and aligned polyaniline (PANI) (Chemical structures of the various polymer and dopant acronyms listed in the manuscript are shown in Supplementary Fig. S1), charge conduction is dominated by metallic transport in the direction parallel to the alignment of the long axis of the polymer chains while a hopping mechanism dominates in the perpendicular direction.^{14, 15}

In addition to the transport mechanism, it is not always clear which type of charge carriers dominate the transport. For example, it has been suggested that both electrons and holes contribute significantly to transport in highly *p*-doped PANI and polypyrrole.⁴ In general, understanding the thermoelectric (TE) effect (and specifically the Seebeck coefficient) in PANI was a subject of interest throughout the 1990s that highlighted the complicated nature of charge-carrier transport in CPs.^{6, 14-16} To accelerate the development of doped CPs across a range of applications, including thermoelectrics and semiconducting devices, it is critical that a robust understanding of charge-carrier transport in these systems be established.

The Seebeck coefficient (or thermopower), which is a measure of the thermoelectric voltage across a material induced by a temperature gradient, can shed additional light on charge-carrier transport in CPs, as it is determined by the average energy of the charge carriers contributing to transport relative to $E_{\rm F}$. As such, Seebeck coefficient measurements have been used to quantify energetic disorder in CPs and help understand transport mechanisms.^{3, 15, 17-19} Furthermore, the Seebeck coefficient is an important parameter in determining the performance of a TE material, as characterized by the figure of merit, $ZT = \frac{\sigma \alpha^2}{\kappa} T = \frac{PF}{\kappa} T$. Here, α is the Seebeck coefficient, σ is the

electrical conductivity, T is the absolute temperature, κ is the thermal conductivity, and PF is the power factor.

Currently, CP TEs are of growing interest for low-cost, mechanically flexible devices for energy generation and temperature control based on the Seebeck and Peltier effects. $^{20-23}$ From the perspective of CP TE development, the performance of n-type CPs must be improved to match their p-type counterparts. This need is because a thermoelectric module requires both n- and p-type legs, and currently the power factors of solution processed n-type CPs are over an order of magnitude lower than p-type CPs. $^{24-26}$

In pursuit of better n-type CPs, two groups recently observed that the sign of α changed from negative to positive at high dopant concentrations. These examples used different polymers and different n-type dopants, with Hwang, et~al. Using the dopant NaNap with the polymer P(PymPh) and Liu et~al. Using N-DMBI with PNDI2TEG-2T (see Supplemental Figure 1 for chemical structures). However, in both cases the power factors were relatively low for both n-type and p-type performance ($\leq 0.81~\mu W~m^{-1}~K^{-2}$). These observations lead to two important questions. First, the fundamental question of why does the sign of the Seebeck coefficient change in some polymers upon increasing the dopant concentration? Second, the application relevant question of can this approach be used to create high-performing can These recent observations and the questions they raise bring us back to fundamental questions of charge-carrier transport in CPs.

The observation of α changing sign in CPs or small molecule organic semiconductors occurs sparsely in the literature. 17, 29, 30 The most studied system that can show a change in the sign of α without changing the dopant type is PANI.^{6, 14-16} In PANI, the sign of α can change based on pH,⁶ the degree of crystallinity,²⁹ and even the direction of measurement in aligned PANI samples.¹⁷ This transition from positive to negative α , which primarily occurs upon reducing the temperature, is attributed to the relative contributions of metallic and hopping transport.^{3, 15, 17} Here, the Seebeck coefficient has been modeled as arising due to contributions from both metallic (bandlike) and hopping transport, with the contribution from metallic transport scaling as a_1T and the contribution from hopping transport scaling as $a_0+a_2T^{1/2}$, 3, 15, 17 where all a_X values are constants, and in PANI a_1 and a_2 are of opposite sign.³ In aligned PANI samples, the sign of α is positive when measured in the direction of chain alignment, where metallic conductivity dominates, and negative when measured perpendicular to the direction of chain alignment, 17 where variable range hopping between chains dominates. These previous reports focusing on PANI indicate that there are two distinct transport processes, a metallic-type transport and a hopping-type transport, and that the balance between these processes determines the sign of the Seebeck coefficient.

However, the above literature regarding the Seebeck coefficient in polymers did not directly probe the electron or hole transport and were thus unable to discriminate between electron or hole dominated conduction. As will be explained below, a negative α does not necessarily imply that electrons are the dominant charge carriers. Mateeva *et al.* was the first to suggest that electrons and holes both contribute significantly to

transport in PANI and polypyrrole.⁴ In their work, although α remained positive with varying doping concentration, a model accounting for both electrons and holes in charge transport was adopted to explain the observed relationship between α and σ . Surprisingly, as important as the carrier type is to a fundamental understanding of charge transport in CPs, there has been little definitive proof offered as to the carrier types present in highly doped CPs. Most often the carrier type is simply assumed based on whether the dopant is known to be of p- or n-type. We will show that this is not a safe assumption, as known p-dopants can induce mobile electrons that contribute substantially to charge transport in heavily doped CPs.

Here, we demonstrate that the sign of α in various CPs changes from positive to negative upon increasing the concentration of the ferric chloride (FeCl₃) dopant. In the case of PDPP-4T, we have achieved both a high p-type PF of 24.5 μ W m⁻¹ K⁻² and a high n-type PF of 9.2 μ W m⁻¹ K⁻² using the same FeCl₃ dopant, with 9.2 μ W m⁻¹ K⁻² being a new record for an n-type donor-acceptor (D-A) conjugated polymer. We further explore the origin of this change in the sign of the Seebeck coefficient through ultraviolet and inverse photoelectron spectroscopy (UPS and IPES, respectively), αc -Hall effect measurements, density functional theory (DFT) calculations, electron paramagnetic resonance (EPR), and UV-Vis-near-IR absorbance. The combination of results shows that the densities of occupied and unoccupied states converge as the doping concentration in the sample increases, leading to the reduction of the band gap to zero at high doping levels. With no band gap, holes and electrons populate the occupied and unoccupied manifolds of

states, respectively, and both carrier types contribute significantly to the electrical conductivity.

Results and Discussion

The family of polymers displayed in Fig. 1 was selected owing to their diverse chemical structures, including both homopolymers and donor-acceptor co-polymers, differing morphologies, spanning from fully amorphous to semi-crystalline, differing charge-carrier mobilities, as well as the wide variation in electronic bandgaps, electron affinities (EA), and ionization energies (IE). The UPS, IPES, and UV-Vis absorbance spectra of all pristine polymers, as well as their electronic bandgaps and optical gaps, were measured and are included in Supplementary Fig. S2 and S3 and Table 1, respectively. As shown in Supplementary Table S1, there is good agreement between the electronic and optical gaps, with the optical gaps typically being 0.1 to 0.3 eV smaller than the electronic gaps. Ferric chloride is used as the dopant due to its ability to dope polymers to high doping concentrations.³¹ This choice is important, as larger or less-miscible dopants are not able to reach high doping levels.31,32 The polymers were doped with FeCl3 at doping ratios ranging from 0.019 to 1.5. Here, the doping ratio refers to the ratio of the moles of dopant molecules to the moles of aromatic rings of the polymer. For example, DPP-4T has six aromatic rings in the repeat unit, and a doping ratio of 0.17 corresponds to one dopant molecule per polymer repeat unit.

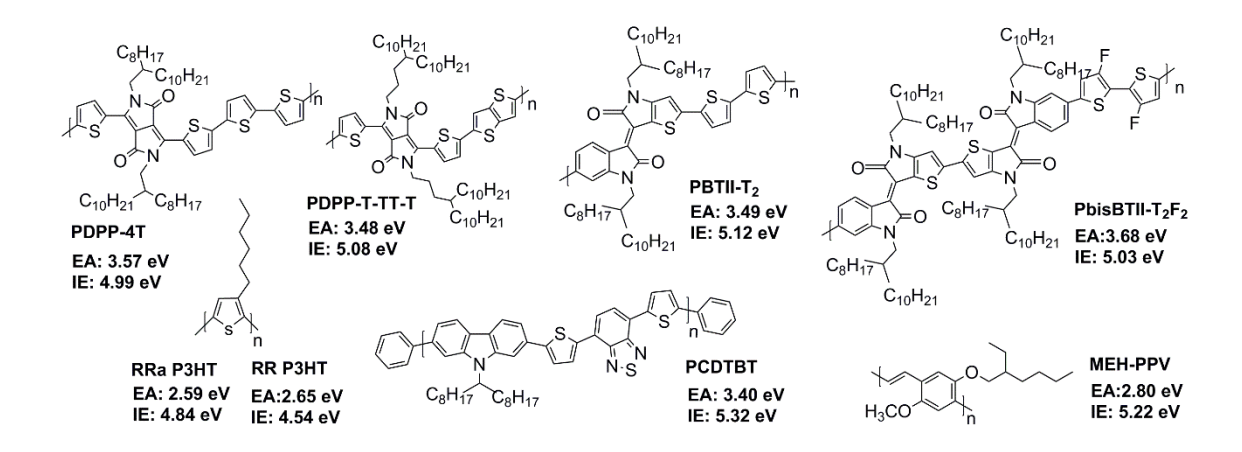
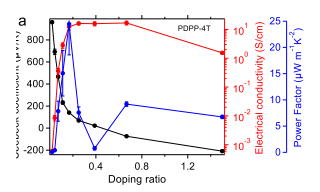
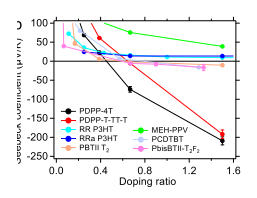


Figure 1: Polymers and their EA and IE values, as measured for the undoped polymers with IPES and UPS, respectively (for details, see Supplementary Fig. S2 and S3 and Table S1).

The first polymer that we focus on is PDPP-4T, as it reaches the highest n-type and p-type PFs among all polymers investigated. At low doping concentrations (Fig. 2a, b), the Seebeck coefficient is positive and decreases with increasing doping concentration, which is the typical behavior for a p-doped material. Similarly, σ increases with increasing dopant concentration. The electrical conductivity plateaus at 16-17 S/cm at doping ratios of 0.25 to 0.67. Here, the UV-Vis-NIR absorbance spectra presented in Supplementary Fig. S3b show that the neutral state absorbance band continues to bleach and the polaron and bipolaron band intensity continue to increase, indicating that the polymer continues to undergo further doping at these high doping concentrations. Over the doping region where σ plateaus, the Seebeck coefficient continues to steadily decrease as it moves from 69 to 22 μ V/K and flips its sign to reach -74 μ V/K. As a result, the power factor changes from a maximum of 25 μ W m⁻¹ K⁻² when α is positive to a maximum of 9.2 μ W m⁻¹ K⁻² when α is negative. This is the first example of a high-

performing TE polymer showing both high p-type and high n-type power factors when only the dopant concentration is varied. Additionally, the n-type power factor is among the highest reported for n-type CPs and the highest of any reported n-type donor-acceptor polymer (Supplementary Table S2).





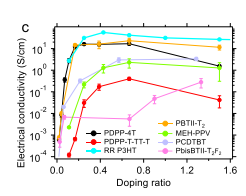


Figure 2. Seebeck coefficient, electrical conductivity, and power factor for PDPP-4T with varying FeCl₃ dopant ratios (a), Seebeck coefficients (b) and electrical conductivities (c) for a series of CPs with varying FeCl₃ doping ratios.

Fundamentally, and for the future design of materials based on highly doped CPs, it is important to identify why α changes sign. The TE effect arises due to the entropically driven diffusion of charge carriers.³³ The magnitude of the Seebeck coefficient α is determined by the average entropy carried per charge carrier, while the sign of α primarily depends on whether charge carriers at energies above or below E_F contribute

more to the electrical conductivity. The Seebeck coefficient can be generally defined by Equation 1,³³ indicating how α is affected by the energy dependence of σ : it is independent of the charge transport mechanism (i.e., band-like or hopping type), material's morphology (i.e., crystalline or amorphous), or its type (i.e., metal or semiconductor).^{25,31}

$$\alpha = -\frac{k}{q} \int \left(\frac{E - E_F}{kT}\right) \frac{\sigma(E)}{\sigma} dE$$
 Equation 1.

The energy dependence of σ , i.e., how charge carriers at different energies contribute to the electrical conductivity, is affected by the DOS distribution, the Fermi distribution function, and the mobility of charge carriers at different energies. Strictly speaking, the sign of α depends on whether carriers above or below E_F transport more entropy, which generally results in α being determined by whether charge carriers above or below $E_{\rm F}$ contribute more to the total electrical conductivity. Defining the transport energy (E_T) as the average energy of the charge carriers that contribute to the electrical conductivity, $E_T = \int E \frac{\sigma(E)}{\sigma} dE$, if E_T lies above (below) E_F then α is negative (positive), as illustrated in Supplementary Fig. S4. One does not need to account for the polarity of the charge carriers; only whether E_T is above or below E_F matters. In a metal, where electrons are the charge carriers, the electrical conductivity arises primarily from the contributions of the large number of mobile electrons at and near E_F ; thereby, the sign of α is typically determined by the sign of $d\sigma/dE$ at $E_{\rm F}$. Notably, electrons are the charge carriers in metals, yet most metals display positive Seebeck coefficients.³⁵ In a doped semiconductor the sign of α commonly depends on whether the material is p- or ndoped, with p- and n-doped materials giving positive and negative Seebeck coefficients, respectively. This trend is simply because in an n-doped material charge carriers above E_F normally contribute more to the total electrical conductivity, while in a p-doped material most mobile charge carriers are located below E_F . However, at high doping levels some semiconductors can start to display a metal-like DOS, and the sign of α may change if the sign of $d\sigma/dE$ changes at E_F . Alternatively, in an organic semiconductor the addition of a chemical dopant may introduce new states for mobile charge-carriers that could lie on the opposite side of E_F relative to the previously dominant charge carriers. 19,21

In CPs, and organic semiconductors in general, the introduction of charge carriers and the presence of ionized chemical dopants result in significant changes to the DOS.³⁶⁻⁴² The large changes to the molecular and electronic conformation upon polaron formation in CPs introduces states that lie at vastly different energies than the electronic states of the undoped organic semiconductor. Previously, the (uncorrelated, paired) hole and/or electron polaron states were both thought to lie in the middle of the gap at the same energy.⁴⁰⁻⁴² As shown recently, however, this model would suggest that it would be easier to oxidize (reduce) the material a second time, in contrast to UPS data that show that the removal (addition) of the second electron is indeed a higher energy process.³⁶⁻³⁹ Density functional theory (DFT) calculations from Heimel resolved this discrepancy by accounting for the spin orbitals, which shift to different energies upon oxidation (reduction) due to Coulombic interactions.³⁸ Notably, in both models doping results in both the electronic band gap and the optical gap being greatly reduced. Due to

the significant changes in the electronic structure of the polymer upon doping, understanding charge transport becomes more complicated and we must account for the altered electronic structure upon doping. DFT calculations on isolated oligomers that represent a subset of five polymers considered experimentally – two homopolymers (MEH-PPV and P3HT) and three donor-acceptor copolymers (PDPP-4T, PDPP-T-TT-T, and PDCTBT) – show that the CPs in this study follow the trends reported by Heimel. The adiabatic ionization energy (AIE; oxidation) follows MEH-PPV < P3HT < PDPP-4T ~ PDPP-T-TT-T < PCDTBT, while the adiabatic electron affinity (AEA; reduction) follows PDPP-T-TT-T > PDPP-4T > PCDTBT > P3HT > MEH-PPV. As shown in Supplementary Table S1 and S3, these results roughly follow the UPS and IPES trends observed for the undoped polymers.

Based on our discussion of the Seebeck coefficient, the change in α observed for PDPP-4T indicates that E_T shifts from below E_F (when α is positive) to above E_F (when α is negative) as the concentration of FeCl₃ is increased. This change could arise from the formation of new mobile states that form upon doping and lie above E_F , or a metal-like DOS with $d\alpha/dE$ at E_F changing from positive at lower doping concentration to negative at high doping concentration. Importantly, this metal-like DOS is not meant to imply metallic transport, only that the DOS resembles that of a metal. Recent work by Liu, et al. supports the formation of new mobile states, while the work of Hwang, et al. supports the metal-like DOS with $d\alpha/dE$ changing sign at E_F . $^{27, 28}$ Liu, et al. explain the change in α of n-doped PNDI2TEG-2T from negative to positive as arising from the increased contribution of electron transport through states that lie at energies below E_F . Here, they contend that at moderate doping concentrations charge-transfer complexes that lie

below E_F begin to dominate transport. This scenario differs from that suggested by Hwang, et al., where the change of α from negative to positive in P(PymPh) upon heavy n-type doping was hypothesized to result from the filling of the LUMO band, which effectively converted the original LUMO into the HOMO upon heavy doping.²⁷ Here, they suggested that the over half-filled new HOMO band (previously the LUMO) with heavy doping resulted in p-type behavior. This explanation is equivalent to treating the material as a metal (or a Fermi glass where $E_{\rm F}$ sits near the middle of a band of electronic states)⁹ with $d\sigma/dE$ at E_F changing from negative to positive upon doping. That is, E_F lies in the middle of a band, as it would for a metal, and the sign of α is negative when there are more states available at energies above E_F (LUMO less than half filled) and changes to positive as E_F shifts upon doping and more states become available below E_F (LUMO over half filled, now defined as the HOMO). In both examples, the DOS and its relationship to E_F is critical. Thus, to probe the change in the energies of the occupied and unoccupied states relative to $E_{\rm F}$ we performed UPS and IPES measurements on PDPP-4T as a function of FeCl₃ loading.

The UPS and IPES data shown in Fig. 3 reveal that the band gap narrows and is essentially eliminated as the doping concentration increases. The undoped sample appears as expected, with E_F falling approximately halfway between the HOMO and LUMO bands and the UPS and IPES data showing a 1.42 eV band gap. As the doping concentration is increased to 0.05, E_F moves closer to the HOMO onset and both the IE and EA increase slightly. Here, the change in the EA is more significant and the band gap is reduced to 1.3 eV. Upon doping at 0.1 mole ratio, the work function increases further

and the HOMO and LUMO bands both shift towards E_F as the bandgap narrows. The band gap reduces to 0.7 eV for the 0.1 doped sample based on a linear fit to the lower third of the main onset region; however, a tail of states in the IPES spectrum extends nearly to E_F and based on this tail the band gap is reduced to only 0.4 eV. The doping ratio of 0.67 leads to a more pronounced signal in the IPES tail region that extends to E_F and a reduced band gap of <0.1 eV. When presented on a semi-logarithmic scale, the sample with 0.67 doping ratio shows that both the occupied and unoccupied states extend to E_F . Qualitatively, the UPS and IPES spectra are most consistent with a semi-metallic DOS at high doping ratios. If E_F was within one band, we would expect more states at E_F and a more rapid increase of both the occupied and unoccupied states occurring near and at E_F . The convergence of the DOS is not unique to PDPP-4T, as UPS and IPES spectra of RR-P3HT and PCDTBT at FeCl₃ doping ratios \geq 0.43, as shown in Supplementary Fig. S5, reveal the same trend.

Unoccupied states from FeCl₃ are also likely contributing to the IPES spectra. To probe whether states on FeCl₃ may be responsible for the IPES signal extending to E_F , we also doped PDPP-4T with NOBF₄. NOBF₄ also results in p-doped PDPP-4T, and PDPP-4T doped with NOBF₄ at a 0.67 doping ratio shows similar UPS and IPES spectra as the FeCl₃ doped sample, as shown in Supplementary Fig. S6. As NO (nitric oxide) will evaporate from the sample after oxidizing the polymer,⁴⁴ the signal near E_F is not from NO. This similarity in spectra near E_F with different dopants supports that the UPS and IPES signals near E_F are primarily from the polymer. Importantly, NOBF₄ doping shows the same

trends in both the absorbance spectra, electrical conductivity, and Seebeck coefficient as the FeCl₃ doped samples (Supplementary Fig. S3c and Fig.S7).

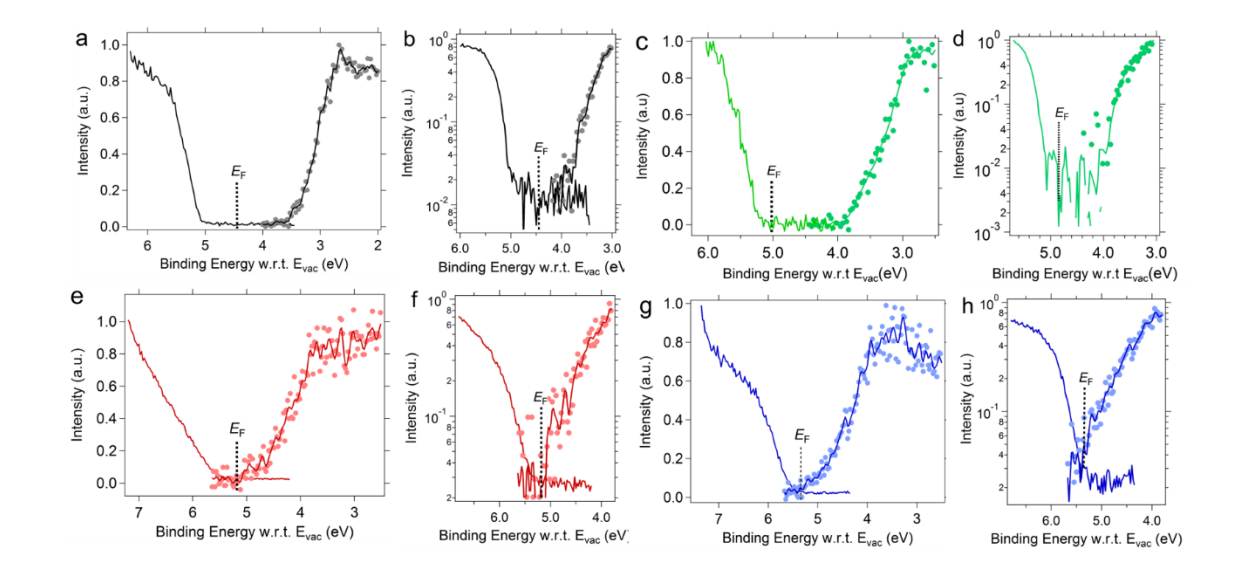


Figure 3: Combined UPS and IPES spectra of PDPP-4T polymer films with 0 (a and b), 0.05 (c and d), 0.1 (e and f), and 0.67 (g and h) doping ratios (defined as the molar ratios of FeCl₃ dopant molecules and the aromatic rings of the polymer). The work functions of the samples are 4.44, 5.02, 5.2, and 5.35 eV for the samples with doping ratios of 0, 0.05, 0.1, and 0.67, respectively. The IPES detector filter energy for PDPP-4T with no dopant is 4.4 eV, 4.88 eV for the 0.05 sample, and 5.8 eV for the 0.1 and 0.67 samples. It is clear from these measurements that the band gap shrinks with increasing concentration of the FeCl₃ *p*-dopant.

To further investigate whether electrons or holes are dominating the charge transport we turn to Hall effect measurements that can reveal the sign of the dominant mobile carriers undergoing a band-like transport. We first verified that the doped polymer samples studied here were not contact limited by performing measurements of

the longitudinal transport via the four-probe technique. The Hall effect studies were performed by using an αc -Hall methodology, recently shown to be indispensable for the studies of the intrinsic charge transport properties of low-mobility systems, such as organic semiconductors. 45, 46 In this method, a low-frequency (< 1.5 Hz) ac magnetic field of a small magnitude (r.m.s. B = 0.23 T), applied perpendicular to the film's plane, is used in combination with a phase-sensitive detection of the corresponding ac-Hall voltage, V_{Hall} , by a lock-in amplifier, while a dc excitation current, I_{SD} , is applied to the film (Fig. 4). This methodology drastically enhances the signal-to-noise ratio in Hall voltage measurements, thus eliminating the need for very high magnetic fields otherwise necessary in Hall measurements of low- μ systems. In our setup, negative or positive inphase component of Hall voltage corresponds to electrons or holes dominating the charge transport, respectively. Such an assignment has been verified by control measurements of pristine rubrene single-crystal OFETs known to operate as p-type FETs⁴⁷, as well as commercially available n-doped Si wafers (Fig. 4). If the in-phase V_{Hall} > 0 were observed in our highly doped polymers, it would indicate that holes are the dominant delocalized charge carriers governing the charge transport, rather than electrons. This observation would be consistent with a metal-like DOS, whereby holes are still the dominant carrier, but the sign of $d\sigma/dE$ would change. On the other hand, if a semi-metal-like DOS is indeed present, we expect that electrons in the unoccupied states would dominate the charge transport, and the observed Hall voltage should be negative, V_{Hall} < 0. Surprisingly, as we show in Fig. 4, Hall effect measurements of PDPP-4T and P3HT highly p-doped with FeCl₃ show a negative Hall voltage, indicative of electrons being the dominant band-like charge carriers moving through the band of unoccupied states. Observation of an electron-type Hall effect in the heavily doped DPP-4T samples (doping ratio of 0.67) is consistent with the carrier sign switch from positive to negative observed in the Seebeck measurements. Interestingly, the PDPP-4T sample with a lower doping ratio of 0.1 and the P3HT sample with a 0.67 doping ratio both show a negative Hall voltage (Supplementary Fig. S8 and Fig. 4, respectively) even though their Seebeck coefficients are positive. Hall effect measurements of samples with even lower doping fractions (< 0.1) failed to detect any Hall signal (Supplementary Fig. S8).

At the first glance, our Hall and Seebeck measurements only partially agree with each other. Indeed, at a doping ratio of 0.1 in PDPP-4T and 0.67 in RR-P3HT the Hall voltage is negative, while α is positive. However, one must keep in mind that: (a) the motion of electrons and holes may be governed by different mechanisms, such as a hopping or a band-like transport, and (b) while both hopping and band-like carriers contribute to the thermoelectric effect (because both are subjected to a drift in the same direction under a temperature gradient), only the band-like carriers experience the classic Lorentz force generated in a magnetic field applied in Hall effect measurements. Thus, mainly the band-like carriers contribute to the Hall effect. We therefore propose that the negative Hall voltages for the 0.1 doped PDPP-4T and 0.67 doped RR-P3HT samples, observed when α is still positive, can be explained by the primary sensitivity of the Hall effect to charge carriers with a band-like character. With holes in the studied system being more localized and moving via hopping, while the electrons being delocalized and moving via a band-like transport, one can have a situation with $V_{\rm Hall} < 0$

and $\alpha > 0$ simultaneously. Thus, it is likely that in the samples with low doping ratios < 0.1, the hopping holes dominate the charge transport, leading to a positive Seebeck coefficient and undiscernible Hall effect. For higher doping ratios of ≥ 0.1 , the contribution of holes diminishes, while delocalized electrons become more prevalent. This scenario is supported by the fact that at low doping (< 0.1), when the Seebeck coefficient is positive, we were unable to detect any Hall effect. Indeed, in the regime dominated by hopping carriers (holes, in this case) no classical Hall effect is expected. Notably, on a macroscale the transport is not band-like, as temperature dependent electrical conductivity measurements (Supplementary Fig. S9) of both PDPP-4T and RR-P3HT fit well with models of hopping type transport. Thus, the band-like transport in this system probably occurs over tens of nms, where the chains are more ordered, and it is likely disrupted by disordered regions.

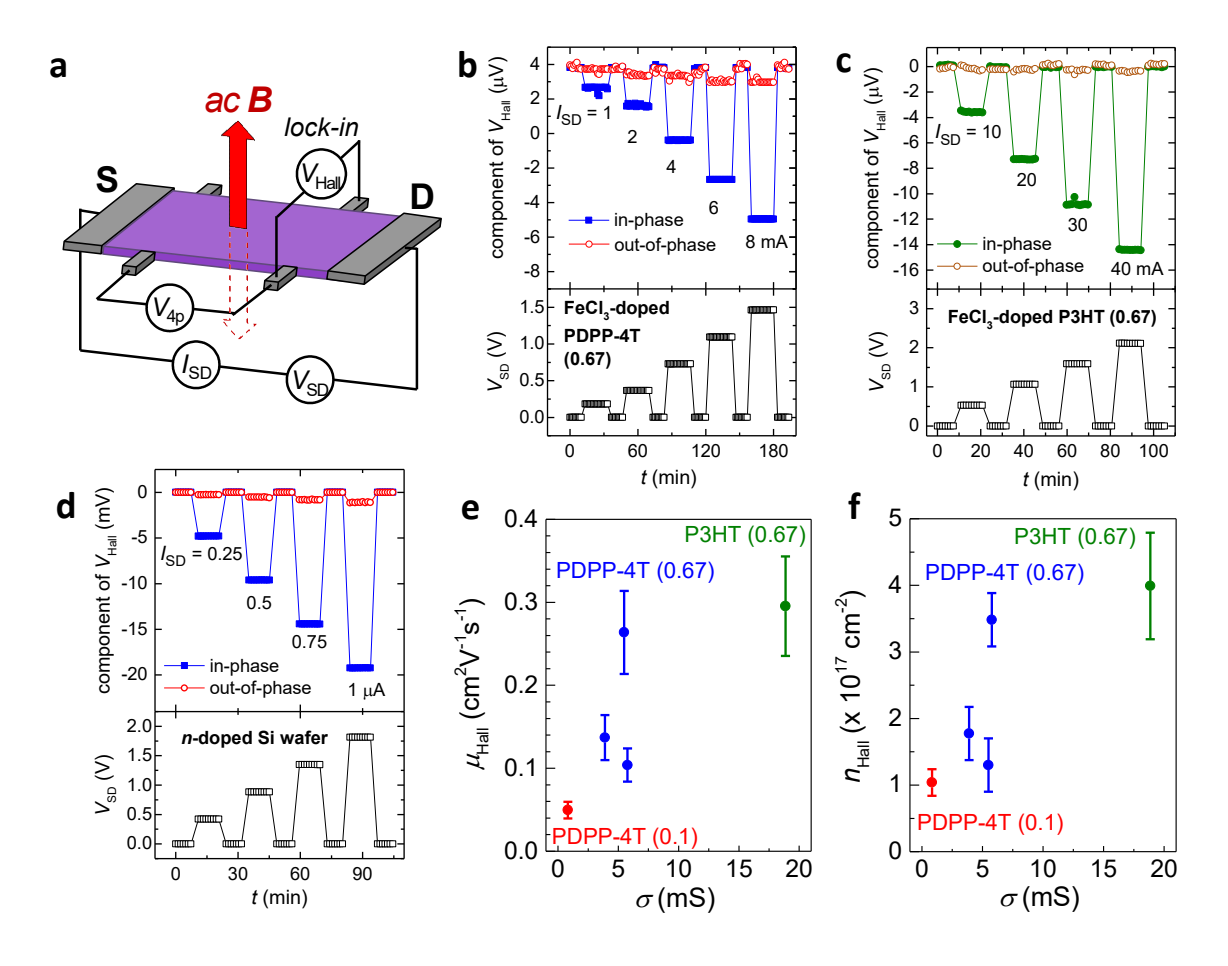


Figure 4. ac-Hall effect measurements of conjugated polymer films heavily doped with FeCl₃ electron acceptor. (a) Schematics of ac-Hall effect measurements using an ac magnetic field, B, oscillating at a frequency f = 0.7 - 0.8 Hz, and an ac Hall voltage, V_{Hall} , detected by a lock-in amplifier, while a longitudinal dc current, I_{SD} , flows between the source (S) and drain (D) contacts. (b) The Hall data for FeCl₃-doped PDPP-4T with a doping ratio of 0.67. (c) The Hall data for FeCl₃-doped P3HT with a doping ratio of 0.67. (d) The control ac-Hall measurements of an n-doped Si wafer to verify the carrier sign assignment. The in-phase and out-of-phase components of V_{Hall} , with the corresponding I_{SD} values indicated, are shown in the upper panels. The "ups" and "downs" in the V_{Hall} signal are due to I_{SD} being switched on and off to establish the zero-current baseline of the Hall voltage. (e) The resultant Hall mobility vs. (projected) conductivity for a collection of all measured polymer samples (each data point is an average of 4 samples from the same fabrication batch). The two 0.67-doped PDPP-4T batches with

 $\mu_{\text{Hall}} = 0.1 - 0.15 \text{ cm}^2\text{V}^{-1}\text{s}^{-1}$ were fabricated at the same time, while the 0.67-doped PDPP-4T batch with $\mu_{\text{Hall}} = 0.25 - 0.3 \text{ cm}^2\text{V}^{-1}\text{s}^{-1}$ was fabricated two months later from a different batch of PDPP-4T. (**f**) The Hall carrier density vs. (projected) conductivity for the same set of samples. The main observation is the negative sign of the in-phase Hall voltage (relatively to the zero-current background) in polymers heavily doped with FeCl₃ electron acceptor, signaling an electron dominant charge transport.

The next question that we address is whether the flip in the sign of the Seebeck coefficient occurs for other highly doped CPs shown in Fig. 1. Fig. 2b shows that for doping ratios of less than 0.5 (i.e., less than 1 dopant molecule per 2 aromatic rings) the Seebeck coefficient remains positive for all conjugated polymers. This positive Seebeck coefficient agrees with the p-type doping mechanism. However, as the doping concentration increases to 0.67 (2 dopant molecules per 3 aromatic rings) the Seebeck coefficient changes its sign from positive to negative in 5 of the 8 polymers investigated. PDPP-T-TT-T and PDPP-4T show the largest negative Seebeck coefficients of $\alpha \approx$ -200 μ V/K, while α for the other polymers remain at α -20 μ V/K. Although many of the polymers show a switch in the sign of α , only PDPP-4T shows a PF above 1 μ W m⁻¹ K⁻².

Besides revealing the carrier type, the Hall effect measurements provide an estimate for the charge carrier mobilities ($\mu_{Hall} = 0.05 - 0.3 \text{ cm}^2\text{V}^-1\text{s}^-1$) and the carrier densities ($n_{Hall} = (0.42 - 1.19) \times 10^{21} \text{ cm}^{-3}$) in these doped polymers (Fig. 4). One should keep in mind though that these values do not necessarily represent the mobility of individual mobile (that is, delocalized) carriers or their actual density. Hall voltage in heavily disordered systems forms as a result of a competition between subpopulations of band-like and hopping carriers, coexisting in a sample.⁴⁶ Therefore, these values can

only be used for relative sample comparison. It's also worth noting that Hall effect measurements carried out earlier in a different CP (PB-TTT), doped with a different strong electron acceptor (F₄-TCNQ), using the same *ac*-Hall apparatus revealed a *p*-type charge transport.⁴⁹ This lends additional credibility to the observation of an electron-type Hall effect in this work, but shows that the emergence of electron conduction in an electron acceptor-doped polymer, although occurring in many systems, still depends on the type of the host matrix, the dopant and the doping level.

The fact that Hall effect measurements do not always show the same carrier type as the Seebeck coefficient agrees with the previous models of charge transport in PANI and its Seebeck coefficient. Here, as discussed in the introduction, the Seebeck coefficient of PANI has been observed to change sign based on the temperature, extent of crystallinity, and measurement direction with respect to the chain alignment. These trends were modeled based on contributions of both metallic and hopping type charge transport, whereby in PANI the contribution of hopping transport to the Seebeck coefficient is negative and that of metallic transport is positive. The combination of our Seebeck coefficient and Hall effect measurements agrees with this model; however, in our samples the band-like contribution to the Seebeck coefficient is negative (*n*-type), and the hopping contribution is positive (*p*-type). To our knowledge, this combination of measurements is the first to provide direct experimental evidence for the presence of both positive and negative charge carriers that move through different transport mechanisms in *p*-doped conjugated polymers.

We additionally note that segregation of FeCl₃ into clusters, with a preferential electron transport through such a phase, can be excluded from the possible mechanisms of the observed electron conduction (for a discussion of control experiments, see Supplementary Information). Briefly, these include the low electric conductivity of pure $FeCl_3$, $FeCl_2/FeCl_3$ blends, $FeCl_3/polyethyleneimine$ blends, and $FeCl_3/Spiro-OMeTAD$ blends (σ < 0.05 S/cm), as well as the control experiments showing that doping PDPP-4T with another p-type dopant NOBF₄ at a 0.67 doping ratio also results in a negative Seebeck coefficient (Supplementary Fig. S7).

Electron paramagnetic resonance (EPR) measurements were conducted on PDPP-4T films doped with FeCl₃ and NOBF₄ through a wide concentration range, as shown in Fig. 5a and Supplementary Fig. S10. The broad peak from pure FeCl₃ leads us to focus on the NOBF₄ doped samples, as undoped NOBF₄ samples show no EPR signal. As the NOBF₄ doping ratio is increased from 0 to 0.015 the EPR peaks at 3462 G and 3465 G increase in intensity, which indicates that unpaired spin states are being generated. From the pre-DFT viewpoint this would be assumed to indicate polaron formation, but DFT calculations have shown that triplet state bipolarons can be more stable and thus these bipolarons will also contribute to the EPR signal. As the doping ratio further increases from 0.025 to 0.39 there is a large decrease in the EPR signal, which indicates that paired spin states are forming. At a doping ratio of 0.39 nearly all spins are paired, as the EPR signal is only 1% of what it was at a 0.025 doping ratio. This concentration corresponds to two dopant molecules per 5 aromatic rings, which is close to the length of a repeat unit (6 aromatic rings). We suspect that at this doping concentration a charge of +2*e* is distributed over

each repeat unit. When the doping concentration is further increased to 0.67 the EPR signal intensity increases, indicating that unpaired spins are again being created.

The results presented allow several unambiguous conclusions: 1) the density of occupied and unoccupied states converge in conjugated polymers at high doping levels, 2) the average energy of charge carriers contributing to the electrical conductivity, E_T , shifts from below E_F to above E_F at high p-type doping in many D-A polymers, 3) negative charge-carriers display more band-like character at moderate to high p-doping levels, and 4) negative Seebeck coefficients appear after the spin concentration has increased after reaching a minimum in NOBF₄ doped PDPP-4T. Taking all these factors into account we propose that following bipolaron formation mobile unpaired electrons are introduced that move through the unoccupied states that were largely introduced through bipolaron formation. How exactly this looks is debatable and at present our theoretical models do not have the capacity to accurately model polaron and bipolaron formation in highly doped polymers with dopant ions present. For example, recent DFT calculations used to refine the classical model only accounted for singly charged polaron states and when these DFT-based calculations were extended to multiply charged states the nature of the state (e.g., whether it has a spin or not) was found to strongly depend on the length of the conjugated backbone. 38,51

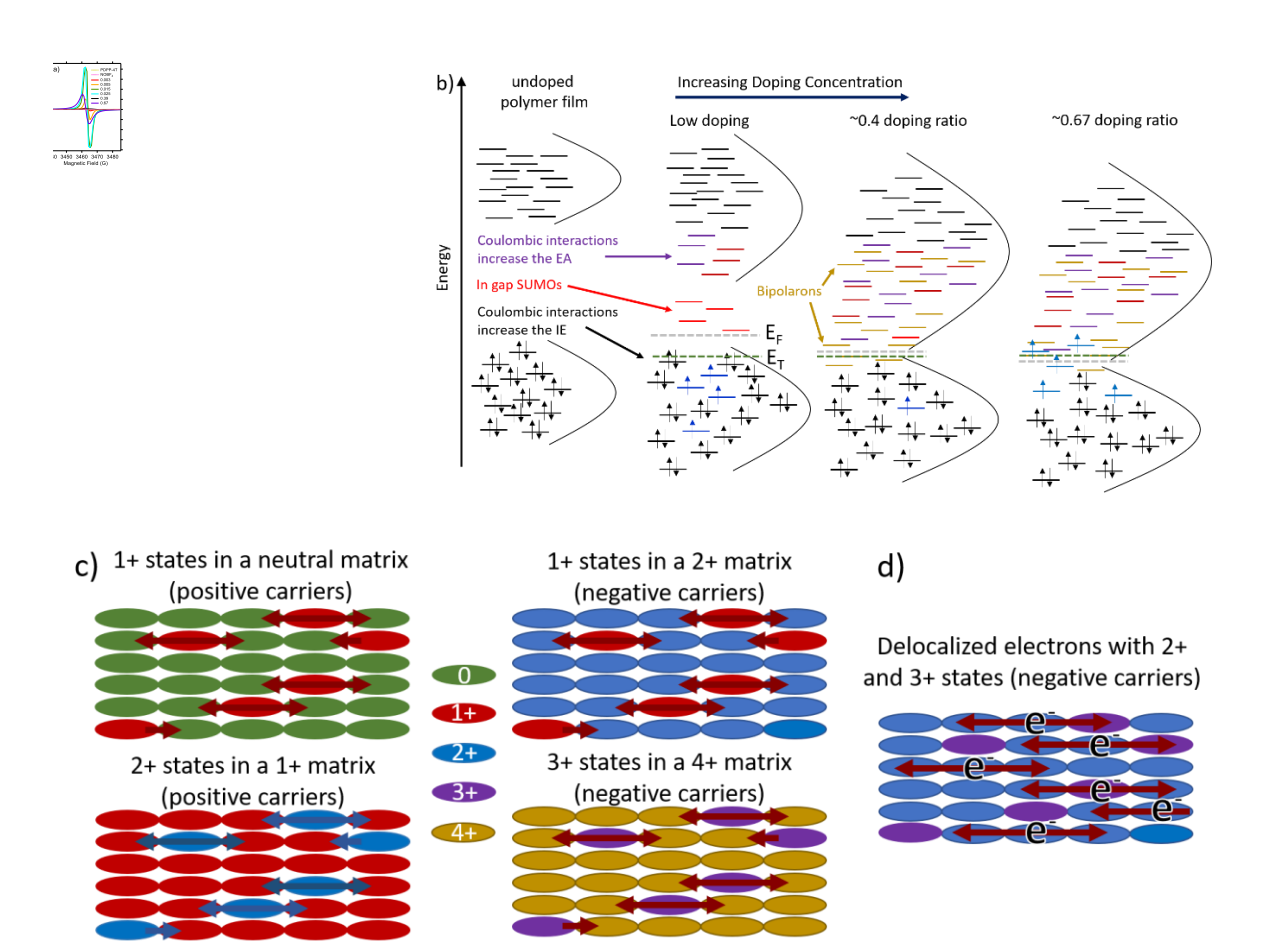


Figure 5. (a) Electron paramagnetic resonance (EPR) of NOBF₄ doped DPP-4T polymers (for each doping sample, 3 mg DPP-4T was used), (b) Density of states schematic showing how Coulombic interactions and orbital splitting result in narrowing of the band gap at high doping concentrations, where SUMO stands for singly occupied molecular orbital, and the two qualitative pictures (c and d) of transport in polymer matrices with varying doping levels.

Two qualitative viewpoints may be adopted based on our results, as illustrated in Figure 5c and d. In the first picture, the additional dopants introduced following bipolaron formation may be rationalized as resulting in the addition of a delocalized electron into the conduction band that is free to move throughout the bipolaron band.

In this picture, a less-mobile 3⁺ state would be introduced while a highly mobile electron moves through the bipolaron (2⁺) band. The second picture is one in which negative charge carriers are transported via 1⁺ charge carriers in a matrix of dominantly 2⁺ states or 3⁺ carriers in a matrix of dominantly 4⁺ states. In such a mechanism the net movement is that of a negative charge carrier.

The notion of high charge states in conjugated polymers has been experimentally and theoretically supported. For example, poly(3,4-ethylenedioxythiophene) has been oxidized to ratios above 0.5 (i.e., more than 1 charge per 2 PEDOT units)⁵⁰ and up to 6 positive charges have been theoretically modeled on a PEDOT dodecamer.⁵¹ Interestingly, recent applications of DFT calculations suggest that the presence of 2 charges does not necessarily result in bipolaron formation and 3 to 6 charges can be coupled in one electronic state on a PEDOT dodecamer. These highly charged states can show less bond length alternation and thereby likely more delocalized transport, which is indeed consistent with our observation of Hall voltages only at high doping concentrations where highly charged states are being formed.

Conclusion

This work highlights the potential of doping conjugated polymers with strong electron acceptors to achieve efficient p- or n-type thermoelectrics, both realized in the same conjugated polymer/dopant system by varying only the concentration of the dopant. Furthermore, traditionally viewed p-type polymers with LUMO levels that make n-type doping difficult can now be investigated for n-type thermoelectric effect through heavy p-type doping. This strategy thereby significantly enriches the potential library of

n-type conjugated polymers for thermoelectric applications. Importantly, several CP/dopant systems demonstrate a change in the sign of the Seebeck coefficient from positive to negative and exhibit an *n*-type Hall effect upon increasing the doping concentration, thus showing the generality of this approach.

Fundamentally, our work builds upon work from the 1990s, whereby positive and negative Seebeck coefficients were observed in PANI. Here, our combined Hall and Seebeck measurements provide direct evidence that both positive and negative chargecarriers contribute significantly to the Seebeck effect, with the positive and negative charge-carriers displaying different extents of dispersive transport. The UPS and IPES measurements show that the occupied and unoccupied states converge upon heavy doping in all the CPs examined, leading to a diminishing band gap and a semi-metal-like DOS. As a result, the sign of the Seebeck coefficient is determined by the carriers that conduct more entropy, which is typically the carrier type that contributes more to the electrical conductivity. The observation that both carrier types can contribute significantly to charge transport in heavily doped CPs, as well as the observation of electrons and holes displaying different degrees of diffusive transport, bring our fundamental understanding of charge carrier transport and TE properties of conjugated polymers at a qualitatively new level, while highlighting that after five decades of research there still remains much to be understood.

Acknowledgements:

K.R.G., Z. L., T.L., A.M.B., and A.A. acknowledge the donors of The American Chemical Society Petroleum Research Fund for partial support of this research (Grant # 57619-DNI10). K.R.G., A.A., and C.R. acknowledge support from the National Science Foundation (DMR-1905734). V.P. and H.H.C. acknowledge support from the National Science Foundation under the grant ECCS-1806363. H.H.C. acknowledges partial support from the Center for Advanced Soft-Electronics at Pohang University funded by the Republic of Korea's Ministry of Science, ICT and Future Planning as Global Frontier Project (CASE-2011-0031628). acknowledges partial support from the Office of Naval Research Young Investigator Program (N00014-18-1-2448). Supercomputing resources on the Lipscomb High Performance Computing Cluster were provided by the University of Kentucky Information Technology Department and the Center for Computational Sciences (CCS). J.M. and X.L. appreciate the support from the NSF (NSF CAREER award number 1653909).

Author contributions

Z. L. and K. R. G. proposed the ideas, designed the experiments, and prepared the manuscript. K. R. G supervised the project. Z. L. carried out the Seebeck coefficient and electrical conductivity measurements and prepared samples for UV-vis-NIR, UPS, IPES, and Hall effect measurements. Z. L., T. L., and A. M. B. performed the UPS and IPES measurements, and A. M. B. helped to build the custom IPES system. H. H. C. and V. P. carried out Hall effect experiments and helped in interpreting the Hall effect data. X. L. and J. M. synthesized diketopyrrolopyrrole polymers and measured the UV-vis-NIR absorbance spectra. U. S. R. and C. R. performed the quantum calculations. J. A. H. and Z.

L. measured electron paramagnetic resonance. D. S., J. L. H. and Z. L. performed the temperature dependent electrical conductivity measurement. A. A. prepared samples and measured electrical conductivities and Seebeck coefficients of FeCl₃ doped Spiro-OMeTAD and wrote the LabVIEW program for the IPES measurements. All authors analyzed data and helped with the writing of the manuscript.

Competing financial interests

The authors declare no competing financial interests.

References:

- 1. Bolto B., McNeill R., Weiss D. Electronic Conduction in Polymers. III. Electronic Properties of Polypyrrole. *Aust. J. Chem.*, **16**, 1090-1103 (1963).
- 2. Chiang C. K., Fincher C. R., Park Y. W., Heeger A. J., Shirakawa H., Louis E. J., et al. Electrical Conductivity in Doped Polyacetylene. *Phys. Rev. Lett.*, **39**, 1098-1101 (1977).
- 3. Joo J., Long S. M., Pouget J. P., Oh E. J., MacDiarmid A. G., Epstein A. J. Charge transport of the mesoscopic metallic state in partially crystalline polyanilines. *Phys. Rev. B*, **57**, 9567-9580 (1998).
- 4. Mateeva N., Niculescu H., Schlenoff J., Testardi L. R. Correlation of Seebeck coefficient and electric conductivity in polyaniline and polypyrrole. *J. Appl. Phys.*, **83**, 3111-3117 (1998).
- 5. Shirakawa H., Louis E. J., MacDiarmid A. G., Chiang C. K., Heeger A. J. Synthesis of electrically conducting organic polymers: halogen derivatives of polyacetylene, (CH). *J. Chem. Soc., Chem. Commun.* 578-580 (1977).
- 6. Park Y. W., Lee Y. S., Park C., Shacklette L. W., Baughman R. H. Thermopower and conductivity of metallic polyaniline. *Solid State Commun.*, **63**, 1063-1066 (1987).
- 7. Wang Z. H., Li C., Scherr E. M., MacDiarmid A. G., Epstein A. J. Three dimensionality of "metallic" states in conducting polymers: Polyaniline. *Phys. Rev. Lett.*, **66**, 1745-1748 (1991).
- 8. Lee K., Cho S., Heum Park S., Heeger A. J., Lee C.-W., Lee S.-H. Metallic transport in polyaniline. *Nature*, **441**, 65-68 (2006).
- 9. Bubnova O., Khan Z. U., Wang H., Braun S., Evans D. R., Fabretto M., et al. Semi-metallic polymers. *Nat. Mater.*, **13**, 190 (2013).
- 10. Wang S., Ha M., Manno M., Daniel Frisbie C., Leighton C. Hopping transport and the Hall effect near the insulator—metal transition in electrochemically gated poly(3-hexylthiophene) transistors. *Nat. Commun.*, **3**, 1210 (2012).
- 11. Chance R. R., Brédas J. L., Silbey R. Bipolaron transport in doped conjugated polymers. *Phys. Rev. B*, **29**, 4491-4495 (1984).
- 12. Zuppiroli L., Bussac M. N., Paschen S., Chauvet O., Forro L. Hopping in disordered conducting polymers. *Phys. Rev. B*, **50**, 5196-5203 (1994).
- 13. Yoon C. O., Reghu M., Moses D., Heeger A. J., Cao Y., Chen T. A., *et al.* Hopping transport in doped conducting polymers in the insulating regime near the metal-insulator boundary: polypyrrole, polyaniline and polyalkylthiophenes. *Synth. Met.*, **75**, 229-239 (1995).
- 14. Yoon C. O., Reghu M., Moses D., Cao Y., Heeger A. J. Thermoelectric power of doped polyaniline near the metal-insulator transition. *Synth. Met.*, **69**, 273-274 (1995).
- 15. Hundley M. F., Adams P. N., Mattes B. R. The influence of 2-acrylamido-2-methyl-1-propanesulfonic acid (AMPSA) additive concentration and stretch orientation on electronic transport in AMPSA-modified polyaniline films prepared from an acid solvent mixture. *Synth. Met.*, **129**, 291-297 (2002).
- 16. Brault D., Lepinoy M., Limelette P., Schmaltz B., Van F. T. Electrical transport crossovers and thermopower in doped polyaniline conducting polymer. *J. Appl. Phys.*, **122**, 225104 (2017).
- 17. Holland E. R., Monkman A. P. Thermoelectric power measurements in highly conductive stretch-oriented polyaniline films. *Synth. Met.*, **74**, 75-79 (1995).
- 18. Venkateshvaran D., Nikolka M., Sadhanala A., Lemaur V., Zelazny M., Kepa M., et al. Approaching disorder-free transport in high-mobility conjugated polymers. *Nature*, **515**, 384 (2014).
- 19. Thomas E. M., Popere B. C., Fang H., Chabinyc M. L., Segalman R. A. Role of Disorder Induced by Doping on the Thermoelectric Properties of Semiconducting Polymers. *Chem. Mater.*, **30**, 2965-2972 (2018).

- 20. Beretta D., Neophytou N., Hodges J. M., Kanatzidis M. G., Narducci D., Martin- Gonzalez M., et al. Thermoelectrics: From history, a window to the future. *Materials Science and Engineering: R: Reports* (2018).
- 21. Glaudell A. M., Cochran J. E., Patel S. N., Chabinyc M. L. Impact of the Doping Method on Conductivity and Thermopower in Semiconducting Polythiophenes. *Adv. Energy Mater.*, **5**, 1401072-n/a (2015).
- 22. Gupta S. K., Jha P., Singh A., Chehimi M. M., Aswal D. K. Flexible organic semiconductor thin films. *J. Mater. Chem. C*, **3**, 8468-8479 (2015).
- 23. Mei J., Bao Z. Side Chain Engineering in Solution-Processable Conjugated Polymers. *Chem. Mater.*, **26**, 604-615 (2014).
- 24. Shi K., Zhang F., Di C.-A., Yan T.-W., Zou Y., Zhou X., et al. Toward High Performance n-Type Thermoelectric Materials by Rational Modification of BDPPV Backbones. *J. Am. Chem. Soc.*, **137**, 6979-6982 (2015).
- 25. Bubnova O., Khan Z. U., Malti A., Braun S., Fahlman M., Berggren M., et al. Optimization of the thermoelectric figure of merit in the conducting polymer poly(3,4-ethylenedioxythiophene). *Nat. Mater.*, **10**, 429 (2011).
- 26. Fan Z., Li P., Du D., Ouyang J. Significantly Enhanced Thermoelectric Properties of PEDOT:PSS Films through Sequential Post-Treatments with Common Acids and Bases. *Adv. Energy Mater.*, **7**, 1602116 (2017).
- 27. Hwang S., Potscavage W. J., Yang Y. S., Park I. S., Matsushima T., Adachi C. Solution-processed organic thermoelectric materials exhibiting doping-concentration-dependent polarity. *PCCP*, **18**, 29199-29207 (2016).
- 28. Liu J., Ye G., Zee B. v. d., Dong J., Qiu X., Liu Y., et al. N-Type Organic Thermoelectrics of Donor–Acceptor Copolymers: Improved Power Factor by Molecular Tailoring of the Density of States. Adv. Mater., **30**, 1804290 (2018).
- 29. Telang P., Mishra K., Prando G., Sood A. K., Singh S. Anomalous lattice contraction and emergent electronic phases in Bi-doped \${\mathrm{Eu}} {2}{\mathrm{Ir}} {2}{\mathrm{O}} {7}\$. Phys. Rev. B, **99**, 201112 (2019).
- 30. Chaikin P. M., Kwak J. F., Jones T. E., Garito A. F., Heeger A. J. Thermoelectric Power of Tetrathiofulvalinium Tetracyanoquinodimethane. *Phys. Rev. Lett.*, **31**, 601-604 (1973).
- 31. Liang Z., Zhang Y., Souri M., Luo X., Boehm Alex M., Li R., et al. Influence of dopant size and electron affinity on the electrical conductivity and thermoelectric properties of a series of conjugated polymers. J. Mater. Chem. A, 6, 16495-16505 (2018).
- 32. Schlitz R. A., Brunetti F. G., Glaudell A. M., Miller P. L., Brady M. A., Takacs C. J., et al. Solubility-Limited Extrinsic n-Type Doping of a High Electron Mobility Polymer for Thermoelectric Applications. *Adv. Mater.*, **26**, 2825-2830 (2014).
- 33. Fritzsche H. A general expression for the thermoelectric power. *Solid State Commun.*, **9**, 1813-1815 (1971).
- 34. Xu B., Verstraete M. J. First Principles Explanation of the Positive Seebeck Coefficient of Lithium. *Phys. Rev. Lett.*, **112**, 196603 (2014).
- 35. Rowe D. M. CRC Handbook of Thermoelectrics. CRC Press, 1995.
- 36. Salzmann I., Heimel G., Oehzelt M., Winkler S., Koch N. Molecular Electrical Doping of Organic Semiconductors: Fundamental Mechanisms and Emerging Dopant Design Rules. *Acc. Chem. Res.*, **49**, 370-378 (2016).
- 37. Winkler S., Amsalem P., Frisch J., Oehzelt M., Heimel G., Koch N. Probing the energy levels in hole-doped molecular semiconductors. *Mater. Horiz.*, **2**, 427-433 (2015).
- 38. Heimel G. The Optical Signature of Charges in Conjugated Polymers. *ACS Central Science*, **2**, 309-315 (2016).

- 39. Png R.-Q., Ang M. C. Y., Teo M.-H., Choo K.-K., Tang C. G., Belaineh D., et al. Madelung and Hubbard interactions in polaron band model of doped organic semiconductors. *Nat. Commun.*, **7**, 11948 (2016).
- 40. Bredas J. L., Street G. B. Polarons, bipolarons, and solitons in conducting polymers. *Acc. Chem. Res.*, **18**, 309-315 (1985).
- 41. Braun S., Salaneck W. R., Fahlman M. Energy-Level Alignment at Organic/Metal and Organic/Organic Interfaces. *Adv. Mater.*, **21**, 1450-1472 (2009).
- 42. Bubnova O., Crispin X. Towards polymer-based organic thermoelectric generators. *Energy Environ. Sci.*, **5**, 9345-9362 (2012).
- 43. Schwarze M., Gaul C., Scholz R., Bussolotti F., Hofacker A., Schellhammer K. S., et al. Molecular parameters responsible for thermally activated transport in doped organic semiconductors. *Nat. Mater.*, **18**, 242-248 (2019).
- 44. Guerrero A., Boix P. P., Marchesi L. F., Ripolles-Sanchis T., Pereira E. C., Garcia-Belmonte G. Oxygen doping-induced photogeneration loss in P3HT:PCBM solar cells. *Sol. Energy Mater. Sol. Cells*, **100**, 185-191 (2012).
- 45. Chen Y., Yi H. T., Podzorov V. High-Resolution ac Measurements of the Hall Effect in Organic Field-Effect Transistors. *Physical Review Applied*, **5**, 034008 (2016).
- 46. Yi H. T., Gartstein Y. N., Podzorov V. Charge carrier coherence and Hall effect in organic semiconductors. *Scientific Reports*, **6**, 23650 (2016).
- 47. Podzorov V., Menard E., Rogers J. A., Gershenson M. E. Hall Effect in the Accumulation Layers on the Surface of Organic Semiconductors. *Phys. Rev. Lett.*, **95**, 226601 (2005).
- 48. Wang S., Ha M., Manno M., Daniel Frisbie C., Leighton C. Hopping transport and the Hall effect near the insulator—metal transition in electrochemically gated poly(3-hexylthiophene) transistors. *Nat. Commun.*, **3**, 1210 (2012).
- 49. Fujimoto R., Watanabe S., Yamashita Y., Tsurumi J., Matsui H., Kushida T., et al. Control of molecular doping in conjugated polymers by thermal annealing. *Org. Electron.*, **47**, 139-146 (2017).
- 50. Rudd S., Franco-Gonzalez J. F., Kumar Singh S., Ullah Khan Z., Crispin X., Andreasen J. W., et al. Charge transport and structure in semimetallic polymers. *J. Polym. Sci., Part B: Polym. Phys.*, **56**, 97-104 (2018).
- 51. Zozoulenko I., Singh A., Singh S. K., Gueskine V., Crispin X., Berggren M. Polarons, Bipolarons, And Absorption Spectroscopy of PEDOT. *ACS Applied Polymer Materials*, **1**, 83-94 (2019).